Time-integrated Channel Response to Tectonic Perturbations in the Deepwater Niger Delta: Implication for Channel Incision and Reservoir Facies Distribution

[1]Byami A. Jolly and [2]Sofolabo O. Adekunle
[1]Department of Geology, Ahmadu Bello University, Zaria - Nigeria
[2]Geophysics Research Unit, University of Port Harcourt, Rivers State, Nigeria

ABSTRACT

Gravity-driven structures in deepwater settings such as the Niger Delta, exert a significant control on sediment gravity flows because they create and determine the location and configuration of sediment depocentres and transport systems. However, to fully understand the interaction between sediment gravity flows and seabed topography we need to evaluate and quantify the geomorphic response of submarine channels to deformation in such areas which in turn, will provide better insight into the distribution of reservoir facies in those settings. This study combines seismic and geomorphic techniques to quantitatively investigate how the growth of thrust-related folds has influenced incision and pathways of Plio-Pleistocene deepwater channel systems in the Niger Delta. Results of this study documents the history of tectonic perturbations since 12.8 Ma and the commensurate impact on submarine channels that develops coevally with the growing structures. The impact of tectonic perturbations on the bathymetric long profiles of these channels is also documented and has provided great insight on how channels appear to respond to variations in substrate uplift rate. Channel incision across growing structures is achieved through enhanced bed shear stress-driven incision (up to 200 Pa) and flow velocity (up to 5 m s-1). Comparison of structural uplift since 1.7 Ma, and channel incision over an equivalent period, showed that these channels are able to keep pace with the time-integrated uplift since 1.7 Ma; and may have reached a topographic steady-state with respect to the structural uplift. This study also provided great insight into the temporal evolution of reservoir facies and their potential organization into hydrocarbon traps as they interact with growing structures through time.

Key words: Channel incision, Tectonic perturbations, Reservoir facies, Channel container, Niger Delta..

INTRODUCTION

Continuous structural deformation and repeated turbiditic flows can generate channel cut-and-fill sequences over time, which can be preserved or partially preserved if channel aggradation dominates (Mayall *et al* 2006; Deptuck *et al.,* 2007; McHargue *et al.,* 2011). Consequently, the channel system fill and geometry should record the history of tectonic perturbations if the resolution of the seismic data is good enough to allow the mapping and analysis of these systems (see Jolly et al., 2016; Pizzi *et al.,* 2023). Despite our knowledge about the tectonic control on submarine channel morphology and architecture, we are yet to fully constrain the spatio-temporal complexity associated with these systems over longer periods and how it impacts the time-integrated distribution of reservoir facies in deepwater settings such as the Niger Delta. A number of studies have analysed channel facies and the overall geometry of submarine channel complexes in terms of how they develop and fill over time (e.g., Mayall and Stewart, 2000; Mayall *et al.,* 2006; Deptuck *et al.,* 2003, 2007). For example, Mayall and Stewart (2000) and Mayall et al. (2006) reported that the channel system fill is made up of several cut-and-fill sequences that are stacked both laterally and vertically through time – and have been referred to as '3rd order' channel complex systems (up to 4 km wide and 150 m thick). Other studies have tended to focus on the impact of tectonic perturbations on channel profiles (e.g., Pirmez *et al.,* 2000; Huyghe *et al.,* 2004; Ferry *et al.,* 2005; Heinio and Davies, 2007; Cavault *et al.,* 2011). However, one key limitation of these studies is that they do not explicitly analyse the relationship between tectonic perturbations and the time-integrated reservoir facies distribution.

Thus, this study is aimed at improving our understanding of the evolution of seabed/near seabed structures and their impact on the evolution of submarine channels that develop coevally with the structural deformation. The study also aims at understanding how the tectonic perturbations have influenced the time-integrated distribution of reservoir facies within the study area.

The authors wish to thank NNPC Limited, NNPC Upstream Investment Management Services (NUIMS), Shell Petroleum Development Company, Department of Geology, Ahmadu Bello University, Zaria - Nigeria and Geophysics Research Unit, University of Port Harcourt, Rivers State, Nigeria for release of the materials and permission to publish this work.

STUDY AREA AND GEOLOGICAL SETTING

The study area is located in the eastern lobe of the toe-thrust system of the Niger Delta in water depths between 2000 m and 4000 m, and covers an area of 75 km by 35 km (Fig. 1). The Niger Delta forms the seaward-end of a NE – SW oriented failed arm of a rift triple junction called the Benue Trough (Fig. 1) which was formed during the opening of South Atlantic following the separation of Equatorial Africa from South America in Early Cretaceous times (Whiteman, 1982; Mascle *et al.,* 1986; Fairhead and Binks, 1991). The trough was progressively filled with younger post-rift deposits and by Late Eocene times a delta had begun to build across the continental margin (Burke, 1972; Damuth, 1994). The delta covers an approximate area of 140,000 km2 both in subaerial exposure and the associated deepwater slope to basin-floor depositional systems (Whiteman, 1982; Damuth, 1994). The delta extends more than 300 km from apex (landward) to the mouth (seaward), and the maximum vertical thickness of the clastic sediments wedge is up to 12 km (Doust and Omatsola, 1990; Damuth, 1994, Morgan, 2004). Major structural zones developed on the delta, and were first sub-divided into three zones by Damuth (1994); and subsequently, Corredor et al. (2005) sub-divided them into five zones. These zones include; (1) the extensional province on the shelf (2) a mud diapir zone located beneath the upper continental (3) an inner fold and thrust belt – characterised by basinward-verging imbricate thrust belt and associated folds including some detachment folds (4) a transitional detachment fold zone beneath the lower continental slope and (5) an outer fold and thrust belt (where the study area occur) in the deepwater end – characterised by both basinward and landward verging thrusts and associated folds. Stratigraphically, the Niger Delta is divided into three diachronous units of Eocene to Recent age that form a major regressive, offlap sequences named the Akata, Agbada and Benin Formations (Avbovbo, 1978; Evamy *et al.,* 1978; Whiteman, 1982; Doust and Omatsola, 1990; Damuth, 1994; Morgan, 2004). The Benin Formation is absent in offshore deepwater Niger Delta (see also Corredor *et al.,* 2005; Maloney *et al.,* 2010), and hence, the Benin Formation is not present in the study area - only the Akata Formation which overlie the basement, and the Agbada Formation which is also structurally deformed, are present (Fig. 1b).

Dataset

A time-migrated 3D seismic reflection dataset was provided by Petroleum Geo-Services (PGS) for the study area. The seismic data volume is part of the PGS Nigerian deepwater megasurvey. The data was processed to near zero-phase and is displayed using SEG-Normal polarity where an increase in acoustic impedance is represented by a peak (positive amplitude on seismic sections). The data was migrated using Kirchhoff pre-stack migration and bending ray post-stack migration to generate a 12.5 m by 12.5 m grid with a 4 ms sampling interval and was

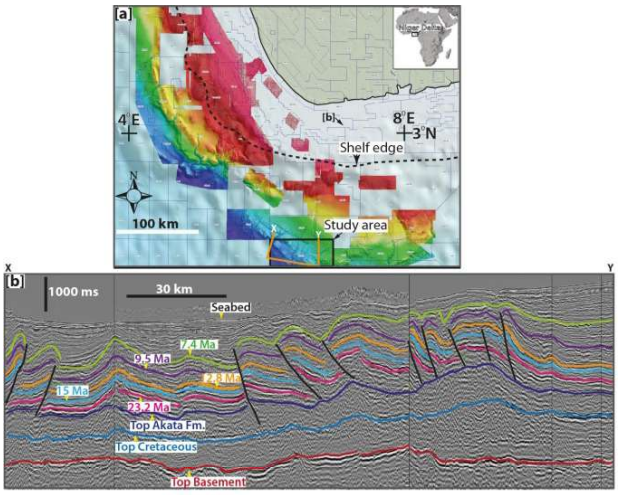

Figure 1: (a) Map of the Niger Delta mega-survey (by PGS) showing the study area located in the toe-thrust region; (b) a tie-line X – Y across the study area (provided by Shell-Nigeria) showing stratigraphic ages and near-seabed structures.

displayed every 4-inlines and cross-lines giving it a bin-size of 50 m which corresponds to the maximum horizontal resolution. The recorded length of the seismic data volume is 9.5 s with a velocity grid of 250 m. Based on the frequency content and assuming an average interval velocity of 2000 ms-1, the data has a vertical resolution of approximately 10 – 12 m in the shallow Plio-Pleistocene section. Calibration of seismic reflections from the 3D survey with age data provided by Shell (Fig. 1b) indicates the upper one second of data (~0.8 to 1 km) below the seabed is of predominantly Pliocene – Recent age. This interval, which is the focus of this study, is characterized dominantly by submarine channels systems (with those studied having an average age of 1.2 – 1.3 Ma, based on analysis using the down-lap surface of the channel levees and an assumption of constant sediment accumulation rate through time).

METHODOLOGY

Measurements of tectonic perturbations (growth of structures) were done using the methodology already documented by Jolly et al. (2016) which is based on the principles of line-length balancing (Dahlstrom,1969) on a series of dip sections spaced at approximately 2 km intervals along the fault-related folds of interest. In order to analyse the evolution of channel systems through time, 3D seismic data was used to map the base and outer-margins of each of the main channel complexes including the currently active channels (here called 'modern channels') and the bounding surface of channel cut-and-fill sequences – including buried systems (here called 'channel container'). It is important to stress that the base of the channel system – i.e. the container base, may be a

composite erosive surface that formed through alternating periods of erosion and partial fill (see Deptuck *et al.,* 2007). The container mapping was conducted using Landmark's 3D seismic interpretation software, from sections taken perpendicular to and along the channel, in order to manually map the erosive surface. This erosive surface was clearly recognised from seismic horizon truncation against the channel cut-and-fill system, and by differentiating the channel fill (which comprises the chaotic base-channel axis seismic reflections (lags and slumps), and the continuous, low-amplitude internal levee seismic reflections) from the truncated seismic reflections of the pre-channel substrate. For each channel system, the container and the associated active channel, where present, were mapped down-system and across growing structures. Using Landmark's interpolation algorithm, continuous container horizons were produced using the manually-picked horizons as seed points. These container horizons were depth-converted using an average seismic velocity of 1700 ms-1 as representative for the channel fill. A thickness map of the container fill in each of the channel systems could then be estimated. For containers whose modern channel is still active, the fill thickness along the container centreline is calculated as the container depth minus the modern channel incision. However, for each buried system, the thickness of the fill is the same as the container depth because the accommodation space created by last period of channel incision prior to abandonment is now filled with abandonment/post-channel deposits. Consequently, the container width measured directly from the thickness map of the buried container will be the same as the maximum width measured between levee crest in a section across the buried container. However, it is important to realise that the width measured directly from the thickness map of the active container will be slightly lower because it will represent width measured at a depth just above the preserved container fill.

A key limitation of this method of thickness calculation comes from the use of a constant velocity (in this case 1700 ms-1) to calculate thickness of the container fill. Variation of velocity within thicknesses of 300 – 400 m maximum is likely to be small in comparison to the value of velocity of 1700 ms-1 (maximum error may be up to 9%; see Deptuck *et al.,* 2007). Another error source may be due to lateral facies variation in container fill (i.e., sands versus shales). The different lithologies will have different velocities which may introduce error into container depth profiles; so higher frequency undulations in container thalweg profiles should be treated with caution; long profiles have therefore been smoothed using polynomial interpolation in order to address this problem. Container thicknesses shown in this study are considered robust enough for the purpose of describing thickness variations within the container, since the priority is the maximum thickness (i.e., thickness along the container axis). Also, buried systems and structures were identified and mapped using Root-Mean-Square (RMS) amplitude maps and seismic sections. The RMS amplitude was extracted in a 100 ms window shifted c.150 m (~180 ms) from the mapped seabed horizon allowing edges of buried channels and outlines of buried structures to be mapped in plan-view.

For the channel long profiles, the depth-converted horizon for each container or the active channel (with depth measured from the sea-level) was exported in text file (x,y,z) format to Arc-GIS, and geo-referenced to build a 50 m resolution Digital Elevation Model (DEM). These DEMs were then processed to get a flow network of channels by building separate flow networks for each channel system. From the flow networks, stream orders were defined and turned into vectors. To extract channel long profiles, the stream order vector coverage was used to run 'cost-paths' that follow the lines of the lowest values in the DEM along a channel system, starting from a user-defined point upstream. From the DEMs, and the mapped channel networks, the following key variables were extracted and measured:

a. The modern channel and container longitudinal profiles (measured as the elevation of the container centreline from sea level, against down-system distance) for each channel system. The down-system paths, along which the profiles were extracted, were defined automatically by the cost-path algorithm in Arc-GIS. To remove noise and smooth steps in the data, the long profiles were fitted with a high-order polynomial, which could be differentiated to obtain the downstream evolution of the along-channel gradient.

b. Modern channel and Container morphometric parameters which include (i) width – the width measured horizontally between outer levee crests; and (ii) depth – the maximum depth of the modern channel incision and the entire cut-and-fill sequences measured vertically from the outer levee crests to the base of the system; (iii) container fill thickness – the thickness of the preserved fill measured by subtracting the depth of modern channel incision from the container depth (Fig. 2). Note that the container fill thickness of the buried systems is the same as the container depth. All morphometric parameters were measured at approximately 1 km intervals along the individual channels in order to capture as much detail as possible.

RESULTS AND DISCUSSION

Tectonic perturbation and channel positioning

Figure 3a and 3b shows the result of the measurement of fold growth through time. From 23 Ma to 9.5 Ma there is no significant growth but the main growth phase was from 9.5 Ma to 3.7 Ma after which, there is a slow down in the

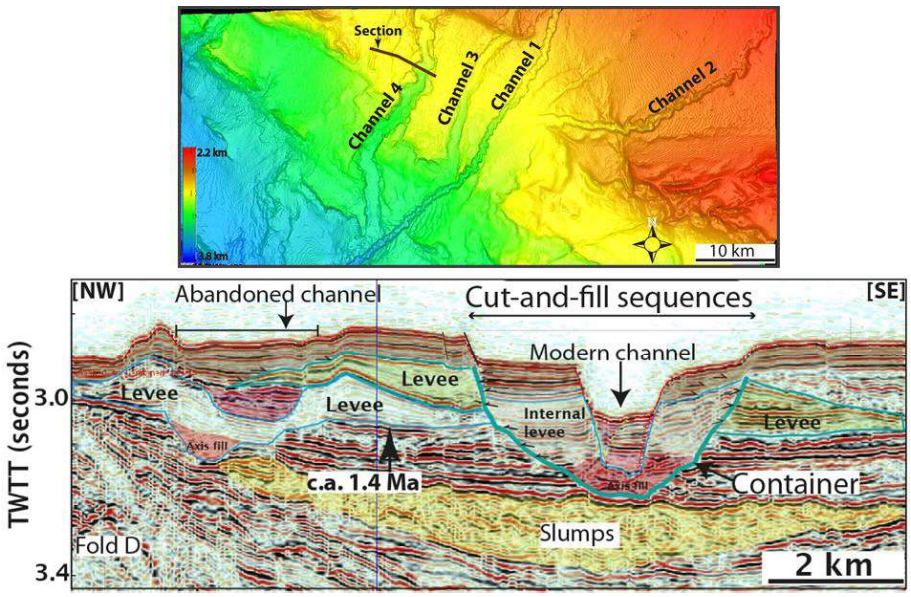

Figure 2: Seismic section across buried channel system and active channel 4 revealing the typical geometry of the channels. Note that modern channels are open to the seabed and the container is made up of several cut-and- fill sequences. The modern channel width is defined by inner levees while the container width is defined by outer levees.

last 3 Myrs. The interval growth rate (i.e. how the growth varies with time; Fig. 3c) also show the main period of growth between 9.5 Ma to 3.7 Ma (see Jolly et al., 2016 for more details). The same pattern of growth was observed in all of the structures studied (Fig. 4), however, the absolute cumulative strain differs from structure to structure. In particular, the green curve (representing growth of Fold C which occurs in the east of the study area) show comparatively lower cumulative strain and interval strain rates. Measurements of near-channel shortening range for the different structures was also carried out in order to compare channel response to tectonic perturbations (Fig. 5). It can be noted that Fold C (represented in green) has the lowest shortening range.

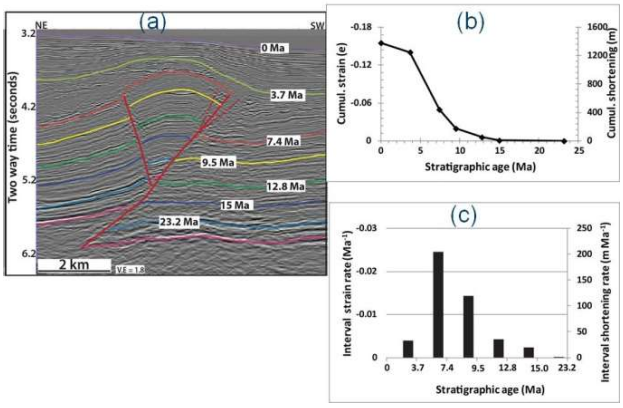

Figure 3: (a) seismic section across a growing fold with stratigraphic ages; (b) cumulative strain or shortening through time and (c) interval strain or shortening.

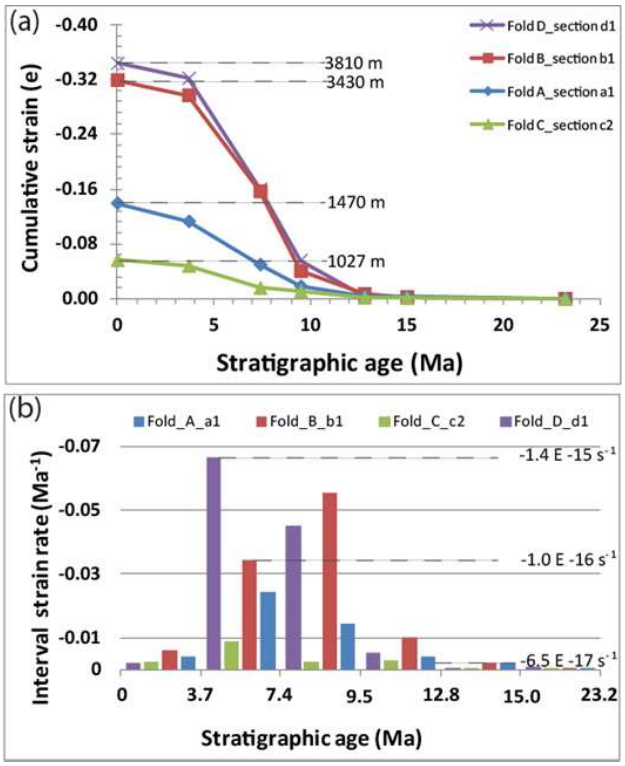

Figure 4: (a) Cumulative strain for all structures studied and (b) Interval strain rate for all structures

In order to determine the positioning channel pathways as they cross these growing structures, the channel paths were plotted on the along strike strain measurments of Fold B (Fig. 6) which shows two bel-shaped curve and a

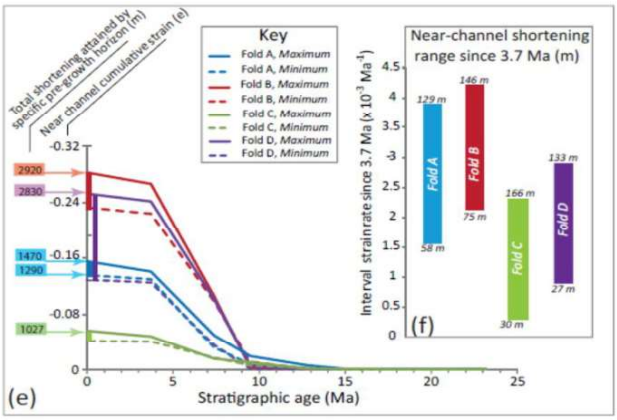

Figure 5: Estimates of near-channel shortening range for all structures. Note that the range for Fold C (green) is the lowest.

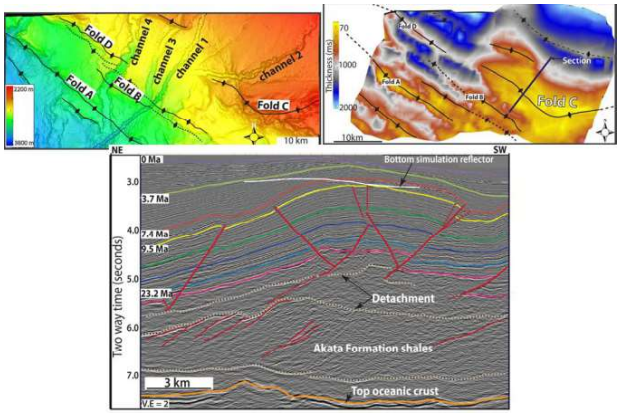

Figure 7: Shows active channel 2 diversion by Fold C despite having the lowest cumulative strain through time

decrease in cumulative strain through time. The channels exploits positions of strain minima in the younger horizons. The growth rate in this interval which also corresponds to the period of channel development is 15 m/Ma. The rate within the older horizons is far greater. This suggests that the interval growth rate within younger stratigraphic horizons at which the channels can keep pace is 15m/Ma; and this is applicable to all structures in the western part of the study area. However, in the east of the study area where Fold C occurs, channels are actively being diverted by this structure (Fig. 7) despite having the lowest near-channel interval growth rate (cf. Fig. 5). Analysis revealed that this particular structure is very broad as demonstared by the Isochron map of the syn-growth interval, thus, the structure behaves more like a detachment fold (see also Maloney *et al.,* 2010).

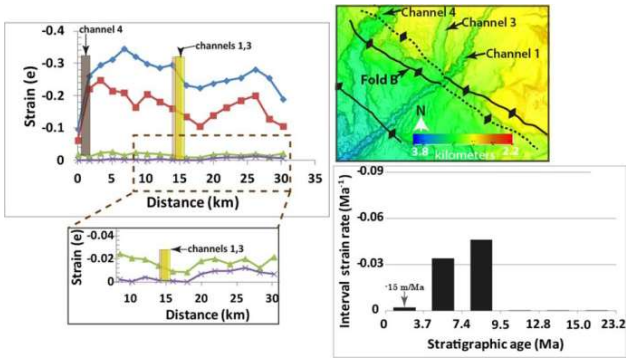

Figure 6: Shows channels positioning as they cross growing structures. Note that the channels exploits areas of minimum strain within the younger stratigraphic horizons that are coeval with channel development.

Geomorphic response to tectonic perturbation

Figure 8 shows the extracted profiles of the modern channels. Here, the active seabed channels have profiles that are generally linear to slightly concave – with concavity up to -0.34, and the average gradient in all channels is ~1o. This linear profiles agrees with previous studies of submarine channels in the Niger Delta (e.g., Pirmez *et al.,* 2000; Cavault *et al.,* 2011). However, in many cases a local increase in gradient corresponds to the positions of underlying thrusts and folds. This regions of increase in gradient are med by corresponding increase in modern channel incision (Fig. 9). This same response is clearly depicted using the histogram shown in Figure 10. Here, we see a mono-modal width distribution for both channels; however, there is a much varied distribution in depth and they tend to be bi-modal as clearly exemplified by channel 2. This varied distribution is the result of the impact of growing structures which causes the channels to respond by increasing incision. Detailed analysis reveals increase in channel incision over growing structures can be up to 50% but the channel width remains relatively constant down-system (Fig. 11a). The aspect ratio of the modern channels (width/channel incision) against downstream gradient shows a large scatter of data points which agrees with reports on aspect ratios of submarine channels by Clark and Pickering (1996); unlike what has been reported for fluvial systems. Estimates of bed-shear stress (power of incision) and flow velocities at those structural locations were found to be up to 200 Pascal (Pa.) and 5 meter per second (m/s) respectively (Fig. 11b). This results agrees with direct observations of turbidites flows (Talling *et al.,* 2012, 2013). In essence, the overall linear nature of the modern channel profiles, the distribution of down-system bed-shear stress, coupled with the fact that the excess channel incision at thrust and fold locations matches the estimated magnitude of structural uplift over a period equivalent to the time of channel development, suggested that these submarine channel systems are capable of maintaining 'topographic steady-state' (see also Pirmez *et al.,* 2000).

To gain a more complete picture of longer-term channel response to on-going deformation, it is therefore

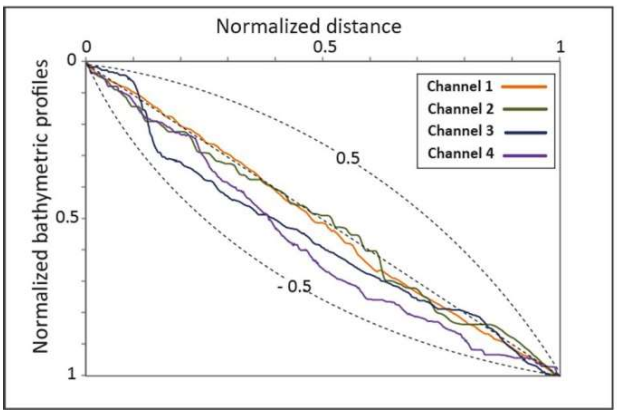

Figure 8: Bathymetric profiles of modern (active) channels. Note that the profiles are linear to concave

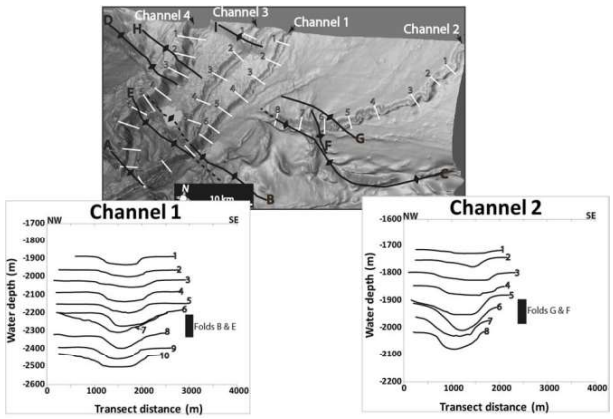

Figure 9: Transects taken across modern channels showing increase channel incision where the channel crosses growing structures.

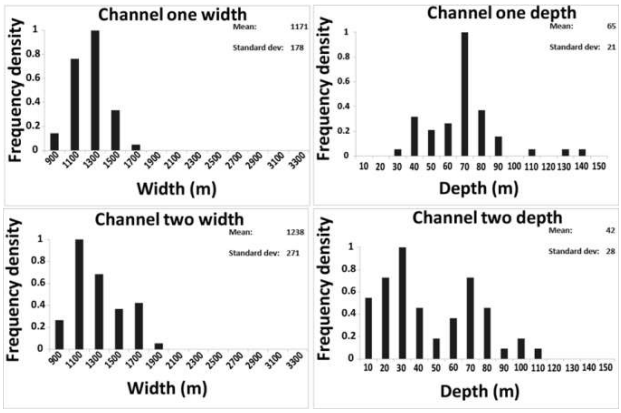

Figure 10: Histogram showing width and depth distribution down-system of channels 1 and 2. Note the mono-modal distribution of width and bi-modal distribution of depths.

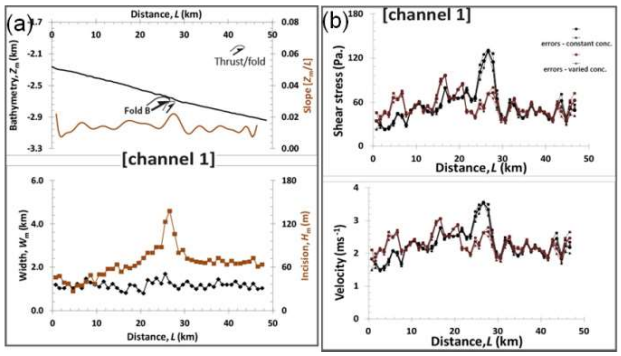

Figure 11: (a) channel 1 profile (upper panel) and width/ incision (lower panel); (b) estimates of channel 1 power of incision (upper panel) and flow velocity (lower panel).

important to analyse the geometry and nature of channel cut-and-fill sequences (containers) that record the time-integrated behaviour of the channel system. Results for the containers show the opposite of what we see in the modern channels (Fig. 12). While the modern channel profiles are generally linear to concave; their associated container profiles are convex to irregular (Fig. 12a). Remember also that the modern channels show no systematic variation in width but for the containers, we do see a slight decrease in the container width in regions where the channels cross active structures and we see also a decrease in the time-integrated container thickness in these zones which also correspond to zones of high channel incision (Fig. 12b). Figure 13 shows a comparison of the modern channel 4 and associated container. The profile for the modern channel is concave while that of the container is convex, and the modern channel incision (erosion) increases over growing folds; however, the preserved container fill in those areas reduces. This suggests that the modern channels are responding to the tectonic perturbations created by the growing folds through incision, and resulting in a concave shape over time. And the container profiles become increasingly convex and irregular due to the time-integrated fold uplift. This suggests that the convex shape of the containers is due deformation; and the concave profile of the modern channels is due to time-integrated incision and erosion over active structure, and hence resulting in lower preserved fill over structural crests.

Tectonic perturbations and reservoir facies distribution

The Seismic facies evolution in the west of the study area (dominated by growing fault-propagation folds) differs from that within a piggyback basin that developed in the east and bounded by a broad detachment Fold C. Distributary channel complexes (splays) are common in the study area, and their deposition is triggered by a sudden increase in seabed gradient (between 0.8o and 4o) at fold tips (R and Y) where incoming channels cut across

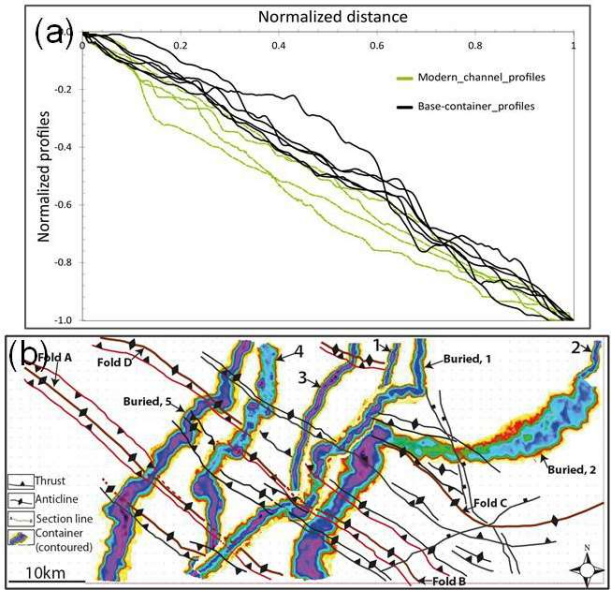

Figure 12: (a) Modern channel profiles (green) and container profiles (black); (b) thickness map of channel containers fill. Note that purple colours show thickness up to 200 m while green colours show thickness less than 100 m.

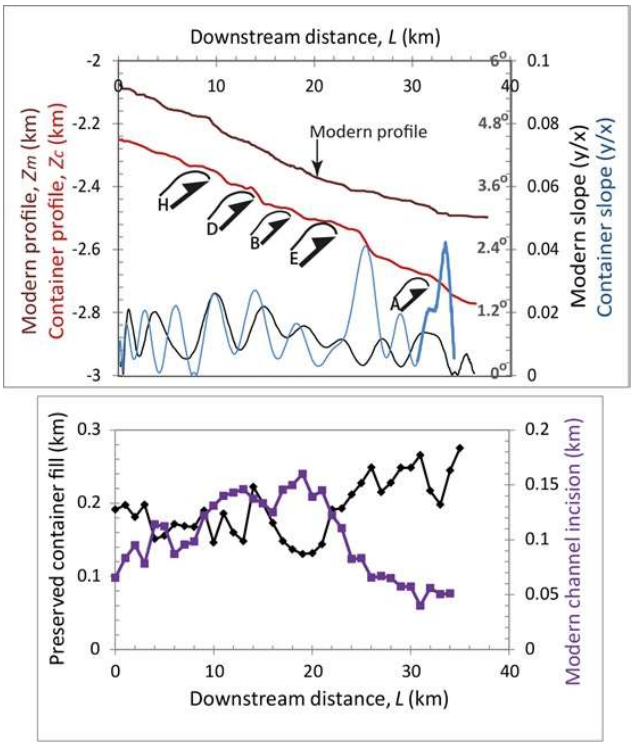

Figure 13: Shows time-integrated channel 4 response to tectonic perturbations. Note that modern channel incision increases but preserved container fill decrease over active structures.

(Fig. 14). The spatial distribution of splays is controlled by the distribution of seabed scarps – located on the forelimbs of growing folds. Splays deposited in sub-basins are lobate-shaped (up to 10 x 15 km). In contrast, splays deposited within the piggyback basin have shapes that are elongated parallel the growing detachment Fold C that is causing the incoming channels to divert (Fig. 15). There are two zone shown in Figure 15 (zone 1 and 2). These two zones illustrate the structural control on splays geometry and architecture. Diversion of channels lead to splays deposition on the outer bend and these splays are elongated parallel to the structure causing the diversion. Over time, the splays (sands) become incorporated into the growing and expanding structure which can forming good trap.

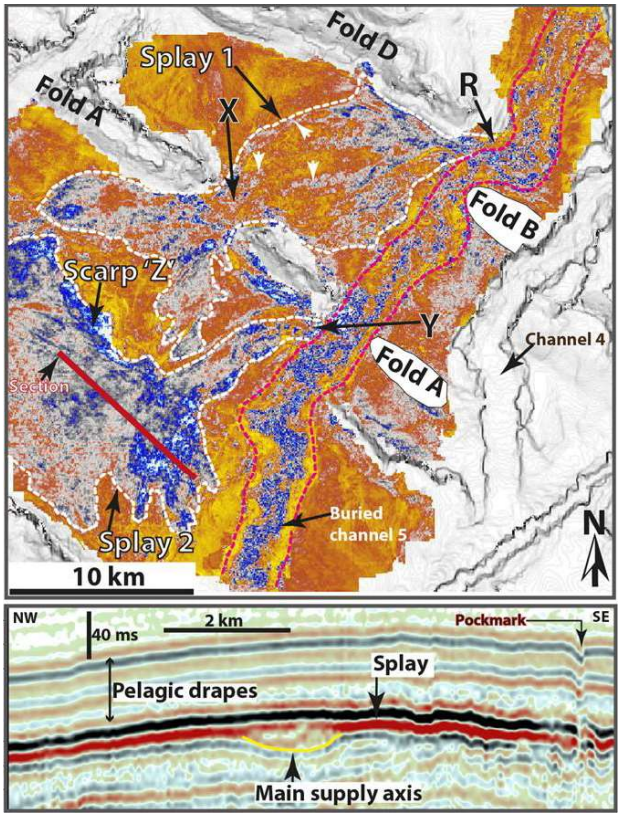

Figure 14: Shows splays development in the western part of the study area. Note that blue colours are high amplitude representing sand deposited within the channel or as splays within mini-basins bounded by growing structures having seabed expression.

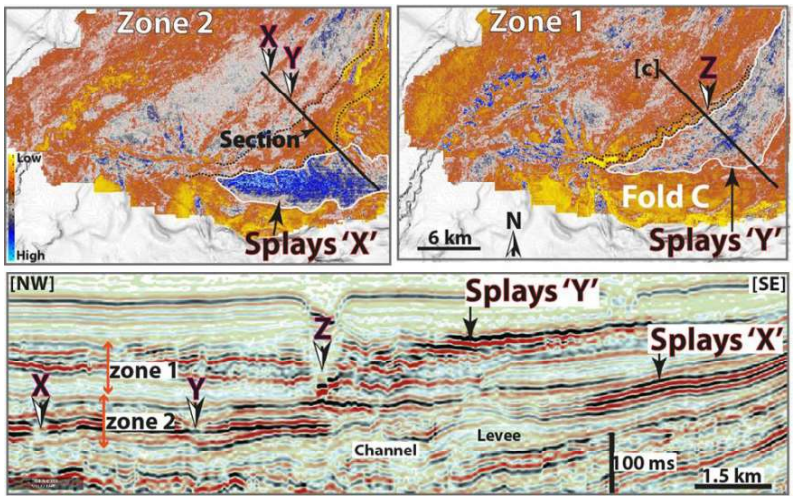

Figure 15: Show splays deposited in the east of the study area where the broad Fold C causes active channel diversion

CONCLUSIONS

This study analyses the time-integrated channel response to tectonic perturbations in the deepwater Niger Delta. Growth of structures having seabed expression was constrained through time with results revealing that Pleistocene channels cut-through structures at points of linkage, where fold shortening rate is < 15 m/Ma. However, broad structures can cause channel diversion even when their shortening rate is comparatively very low.

Modern channels respond to the tectonic perturbations created by growing folds through increase in incision and erosion thus, resulting in a concave shape profile over time. But the associated channel container profiles become increasingly convex and irregular due to the time-integrated fold uplift. Therefore, the convex profile of the containers is the result of time-integrated deformation while the concave profile of the modern channels is due to time-integrated incision and erosion over active structures, and hence resulting in lower preserved fill over structural crests. These observations also suggest that the modern channels are keeping pace with structural growth and therefore, are in a topographic steady-state.

The aspect ratios of the modern channels show large scatter of data points which is in contrast to fluvial systems. However, the opposite was observed for the containers – which show time-integrated narrowing of width over active structures

The time-integrated tectonic perturbations also control the distribution of reservoir facies as seen in the variation of splays geometries in the west and east of the study area characterized by different structural styles.

REFERENCES CITED

Avbovbo, A.A., (1978). Tertiary lithostratigraphy of the Niger Delta. AAPG Bulletin, 62, 295–300.

Burke, K.C.B., (1972). Longshore drift, submarine canyon, and submarine fans. AAPG Bulletin, 56, 1975-1983.

Clark, J.D., Pickering, K.T., (1996)a. Submarine Channels: Processes and Architecture: Vallis Press, London, 231p.

Corredor, F., Shaw, J.H., Bilotti, F., (2005). Structural styles in the deep-water fold and thrust belts of the Niger Delta. AAPG Bulletin, 89, 753-780.

Covault, J.A., Fildeni, A., Romans, B.W., McHarque, T., (2011). The natural range of submarine canyon-and-channel longitudinal profiles. Geosphere, 7, 313-332.

Dahlstrom, C.D.A., (1969). Balanced cross sections. Canadian Journal of Earth Sciences, 6, 743–757.

Damuth, J.E., (1994). Neogene gravity tectonics and depositional processes on the deep Niger Delta continental margin. Marine and Petroleum Geology, 11, 320–346.

Damuth, J.E., Flood, R.D., Knowsmann, R.O., Belderson, R.H., Gorini, M.A., (1988). Anatomy and growth patterns of Amazon deep-sea fan as revealed by long-range side-scan sonar (GLORIA) and high-resolution seismic studies. AAPG Bulletin, 72, 885–911.

Deptuck, M.E., Steffens, G.S., Barton, M., Pirmez, C., (2003). Architecture and evolution of upper fan channel-belts on the Niger Delta slope and in the Arabian Sea. Marine and Petroleum Geology, 20, 649-676.

Deptuck, M.E., Sylvester, Z., Pirmez, C., O'byrne, C., (2007). Migration-aggradation history and 3-D seismic geomorphology of submarine channels in the Pleistocene Benin-major Canyon, western Niger Delta slope. Marine and Petroleum Geology, 24, 406-433.

Doust, H., Omatsola, E., (1990). Niger Delta. In: Edwards, J.D. and Santogrossi, P.A. (Eds.), Divergent /passive margin basins. AAPG Memoir, 48, 201-238.

Evamy, B.D., Haremboure, J., Kamerling, P., Knaap, W.A., Molloy, F.A., Rowlands, P.H., (1978). Hydrocarbon habitat of Tertiary Niger Delta. AAPG Bulletin, 62, 277-298.

Fairhead, J.D., Binks, R.M., (1991). Differential opening of the Central and South Atlantic oceans and the opening of the West African rift system. Tectonophysics, 187, 191–203.

Ferry, J.N., Mulder, T., Parize, O., Raillard, S., (2005). Concept of equilibrium profile in deep water turbidite systems: effects of local physiographic changes on the nature of sedimentary processes and the geometries of deposits, in: Hodgson, D.M. and Flint, S.S. (Eds.), Submarine Slope Systems: Processes and Products. Geological Society London, 244, 181-193.

Heinio, P., Davies, R.J., (2007). Knickpoint migration in submarine channels in response to fold growth, western Niger Delta. Marine and Petroleum Geology, 24, 434-449.

Huyghe, P., Foata, M., Deville, E., Mascle, G., (2004). Channel profiles through the active thrust front of the southern Barbados prism. GSA Bulletin, 32, 429-432.

Janocko, M., Nemec, W., Henriksen, S., Warchol. M, (2013). The diversity of deep-water sinuous channel belts and slope valley-fill complexes. Marine and Petroleum Geology, 41, 7 – 34.

Kolla, V., Posamentier, H.W. and Wood, L.J., (2007). Deep-water and fluvial sinuous channels – Characteristics, similarities and dissimilarities, and modes of formation. Marine and Petroleum Geology, 24, 388-405.

Maloney, D., Davies, R., Imber, J., Higgins, S., King, S., (2010). New insights into deformation mechanisms in the gravitationally driven Niger Delta deep-water fold and thrust belt. AAPG Bulletin, 94, 1401-1424.

Mascle, J., Marhino, M., Wanesson, J., (1986). The structure of the Guinean continental margin: implications for the connections between the Central and South Atlantic Oceans. Geologische Rundschau, 75, 57-70.

Mayall, M., Stewart, I., (2000). The architecture of turbidite slope channels, in: Weimer, P., Slatt, R.M., Coleman, J., Rosen, N.C., Nelson, H., Bouma, A.H., Styzen, M.J., and Lawrence, D.T., (Eds.), Deep-Water Reservoirs of the World: SEPM, Gulf Coast Section, 20th Annual Research Conference, 578 586.

Mayall, M., Jones, E., Casey, M., (2006). Turbidite channel reservoirs – key elements in facies prediction and effective development: Marine and Petroleum Geology, 23, 677–690.

McHargue, T., Pyrcz, M.J., Sullivan, M.D., Clark, J.D., Fildani, A., Romans, B.W., Covault, J.A., Levy, M., (2011). Architecture of turbidite channel systems on the continental slope: patterns and predictions. Marine and Petroleum Geology, 28, 728 –743.

Morgan, R., (2004). Structural controls on the positioning of submarine channels on the lower slopes of the Niger Delta, in: Davies, R.J., Cartwright, J.A., Stewart, S.A., Lappin, M., and Underhill, J.R. (Eds.), 3D seismic technology: application to the exploration of sedimentary basins. Geological Society London Memoirs, 29, 45-51.

Pirmez, C., Beaubouef, R.T., Friedmann, S.J., Mohrig, D.C., (2000). Equilibrium profile and baselevel in submarine channels: examples from Late Pleistocene systems and implications for the architecture of deepwater reservoirs. GCSSEPM Foundation 20th Annual Research Conference, 782-805

Pizzi, M., Whittaker, A.C., Mayal, M., Lonergan, L., (2023). Structural controls on the pathways and sedimentary architecture of submarine channels: New constraints from the Niger Delta. Basin Research, 35, 141 – 171.

Talling, P.J., Masson, D.G., Sumner, E.J., Malgesini, G., (2012). Subaqueous sediment density flows: depositional processes and deposit types. Sedimentology, 59, 1937-2003.

Talling, P.J., Paull, C.K., and Piper, D.J.W., (2013). How are subaqueous sediment density flows triggered, what is their internal structure and how does it evolve? Direct observations from monitoring of active flows. Earth Science Reviews, doi: 10.1016/j.earscirev.2013.07.005.

Whiteman, A.J., (1982). Nigeria: its Petroleum Geology, Resources and Potential: Graham and Trotman, 1, 166p.